CORROSION SCIENCE AND TECHNOLOGY, Vol.9, No.3(2010), pp.122~128

The Effect of Welding Method on the Electrochemical Behavior of Austenitic Stainless Steel Sheet

Young Hune Kim and Kyoo Young Kim†

Pohang University of Science and Technology Department of Materials Science and Engineering San 31, Hyoja-Dong, Nam-gu, Pohang 790-784 Korea

(Received March 25, 2010; Revised June 14 2010; Accepted June 15, 2010)

The corrosion of the flexible tube in the automobile exhaust system is caused by the ambient water and chloride ions. Since welding is one of the key processes for the flexible tube manufacturing, it is required to select a proper welding method to prevent the flexible tube corrosion and to increase its lifetime. There are many studies about the efficiency of the welding method, but no systematic study is performed for the effect of welding method on the corrosion property of the austenitic stainless weldment. The aim of the present study is to provide information on the effect of two different welding methods of TIGW (tungsten inert gas welding) and PAW (plasma arc welding) on the corrosion property of austenitic stainless steel weldment.

Materials used in this study were two types of the commercial austenitic stainless steel, STS321 and XM15J1, which were used for flexible tube material for the automotive exhaust system. Microstructure was observed by using optical microscopy (OM) and scanning electron microscopy (SEM). To evaluate the corrosion behavior, potentiodynamic and potentiostatic tests were performed. The chemical state of the passive film was analyzed in terms of XPS depth profile.

Metallurgical analysis show that the ferrite content in fusion zone of both STS321 and XM15J1 is higher when welded by PAW than by TIGW. The potentiodynamic and potentiostatic test results show that both STS321 and XM15J1 have higher transpassive potential and lower passive current density when welded by PAW than by TIGW. XPS analysis indicates that the stable Cr_2O_3 layer at the outermost layer of the passive film is formed when welded by PAW. The result recommends that PAW is more desirable than TIGW to secure corrosion resistance of the flex tube which is usually made of austenitic stainless steel.

Keywords *: Austenitic stainless steel, STS321, XM15J1, TIGW, PAW*

1. Introduction

The flexible tube of automobile is located between the engine and exhaust system, and used to absorb the vibration. The inner part of the flexible tube is exposed to the hot exhaust gas from the engine, while the outer part of it is exposed to the ambient environment which may contain chloride from the deicing salt. Since the flexible tube is exposed to the dynamic corrosive conditions, the material property of the flexible tube requires a good corrosion resistance in addition to high mechanical strength. Austenitic stainless steel is commonly used for the flexible tube with alloy modification for better corrosion resistance.

Welding is one of the key manufacturing processes for the flexible tube. Tungsten inert gas welding (TIGW) and plasma arc welding (PAW) are generally exercised for manufacturing the austenitic stainless steel flexible tube. When the flexible tube is exposed to the corrosive environment, the weld joint area is preferentially attacked.

The corrosion resistance of the stainless steel mainly depends upon the stability of passive film formed on the surface. However, the stability of passive film may be impaired if welding is not properly controlled. In fact, the field data show that corrosion failure occurs in the weld joint area, or weldment, due to poor stability of passive film.[1)-3)] The stability of passive film in the weldment depends on various welding process parameters as well as the alloy composition of the austenitic stainless steel. Since the thickness of austenitic stainless steel plate used for the flexible tube is as thin as 0.2 mm, there is no heat affected zone which is typical of thick plate welding. The welding method is an important process parameter since it determines the microstructure of the weldment.

† Corresponding author: kykim@postech.ac.kr

In this study, the effect of the welding method on the corrosion property of the flexible tube is investigated. TIGW and PAW are chosen for their commercial importance. The formation characteristics of ferrite phase is examined in terms of different welding process since the ferrite formed in the weldment may play an important role in corrosion process.[4] The passive film stability is evaluated by electrochemical polarization test methods.

2. Experimental procedure

In this study, materials for experiments were employed from one of the pipe forming companies and yield to industrial welding conditions for manufacturing applications. the commercial grade austenitic stainless steels of STS321 and XM15J1 were used and their chemical compositions are listed in Table 1. The plate thickness was 0.2 mm. For welding, butt welding was used, and the welding velocity was fixed at 2.1 m/min. For STS321, the welding current was 22A for TIGW and 1.4A for PAW. For XM15J1, the welding current was 21A for TIGW and 13A for PAW. Argon was used for shielding gas, and backing gas with the flow rate of 10 l/min and 5 l/min, for TIGW and PAW, respectively. Hereafter, the specimens will be denoted by their composition and welding method as STW (STS321, TIGW), SPW (STS321, PAW), XTW (XM15J1, TIGW) and XPW (XM15J1, PAW).

For the microstructural analysis, STS321 was electrolytically etched in 60% HNO_3 solution at 0.4 V for 30 sec. XM15J1 was immersed in 15 ml HCl + 85 ml ethanol for 25 min. After etching, optical microscope (OM) and scanning electron microscope (SEM) were used to evaluate the microstructure.

Potentiodynamic and potentiostatic tests were performed to evaluate the electrochemical behavior of the weldments. All the electrochemical tests were performed at room temperature in ambient air condition. Before potentiodynamic polarizastion test, the specimen was held at -1 V vs. saturated calomel electrode (SCE) for 5 min to remove the oxide scale formed on the specimen surface. Potentiodynamic test was performed by increasing potential from 0.25 V to 1.2 V with respect to open circuit potential (OCP) with the scan rate of 0.5 mV/sec. Potentiostatic test was performed by maintaining at -0.1 V_{SCE} for 1 hr. After potentiostatic test, XPS analysis was performed to obtain the information on the chemical composition of passive film. The sputtering rate was 0.081 nm/sec and Al K (1486.8 eV) was used for the source. Sputtering was graded from level 1 to level 10 with the sputtering time for each level being 15 sec.

3. Results

3.1 Microstructure

Fig. 1 shows the SEM microstructure of weldment. All the specimens are composed of austenite matrix and dispersed ferrite phase. The second phases like $M_{23}C_6$, σ, χ, which are commonly observed from stainless steel, were not detected by the field emission scanning electron microscope (FE-SEM). This may be due to the fact that rapid cooling after butt welding the thin plate does not provide enough time for the formation of the second phases.

3.2 Electrochemical test

Fig. 2 shows potentiodynamic polarization curves. For both STS321 and XM15J1 specimens, the values of OCP are similar, while transpassive potential values of PAW were higher than those of TIGW. Especially, transpassive potential of XPW was 320 mV higher than that of XTW. The passive currents of STS321 are almost the same regardless of the welding methods, whereas the passive current of XM15J1 is lower for PAW than for TIGW. This polarization test suggests that the effect of welding method is more pronounced for XM15J1 than for STS321. The stability of passive film seems to be better with PAW than with TIGW.

The potentiostatic polarization curves shown in Fig. 3 clearly reveal that the stability of passive film is better with PAW than with TIGW. The beneficial effect of PAW is more positively observed from XM15J1 than from STS321.This may come from the fact that after welding the stable passive film of PAW gives high corrosion resistance for local corrosion.

3.3 XPS surface analysis

The results of XPS analyses on the outermost layer of passive film formed on the austenitic stainless steel surface are shown in Figs. 4 and 5. The peak area data are listed

Table 1. Chemical composition of the experimental steel (wt%)

	C	Si	Mn	Ti	S	Cr	Ni	Cu	Mo	N
STS321	0.037	0.41	1.06	0.286	0.0011	18.1	9.20	0.131	0.100	0.0134
XM15J1	0.052	3.42	0.494	0.002	0.0011	20.6	13.7	0.160	0.055	0.0257

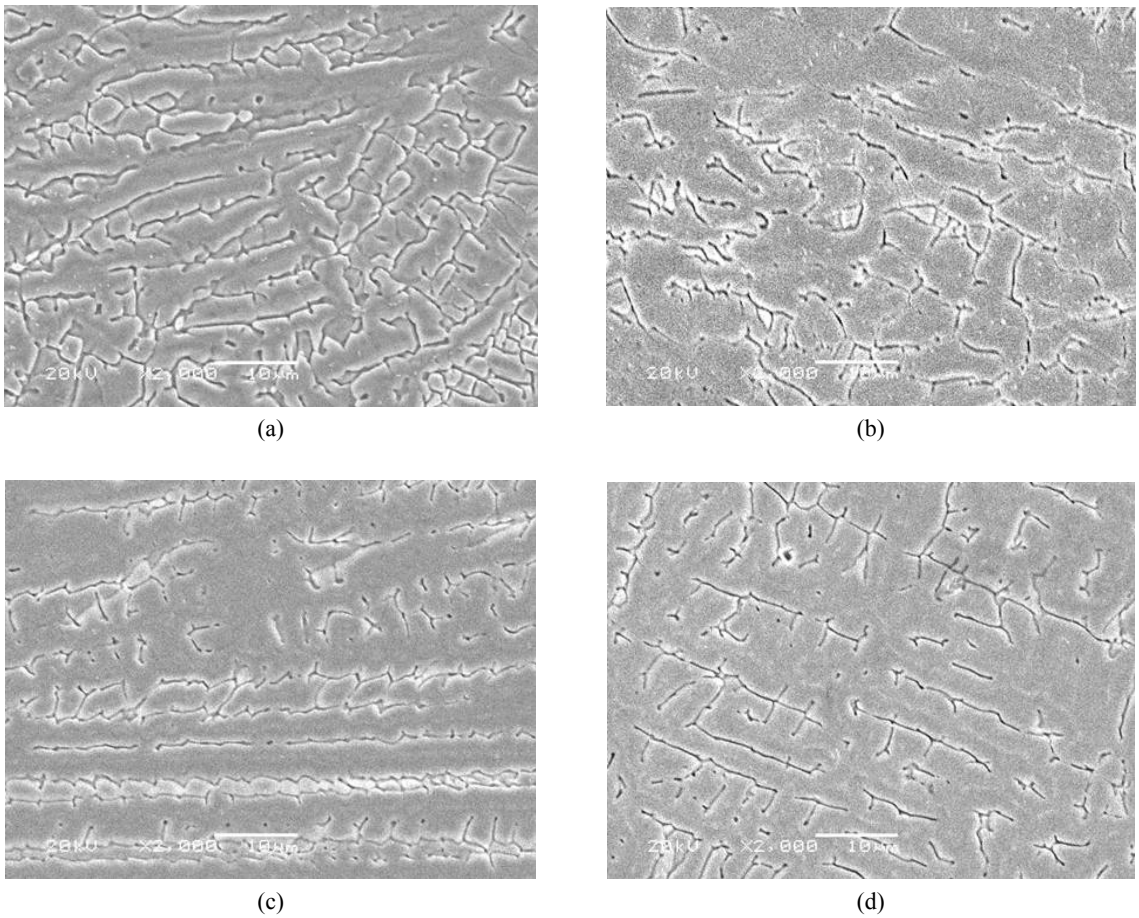

(a) (b) (c) (d)

Fig. 1. SEM photographs of weldment; (a) STW, (b) SPW, (c) XTW, and (d) XPW.

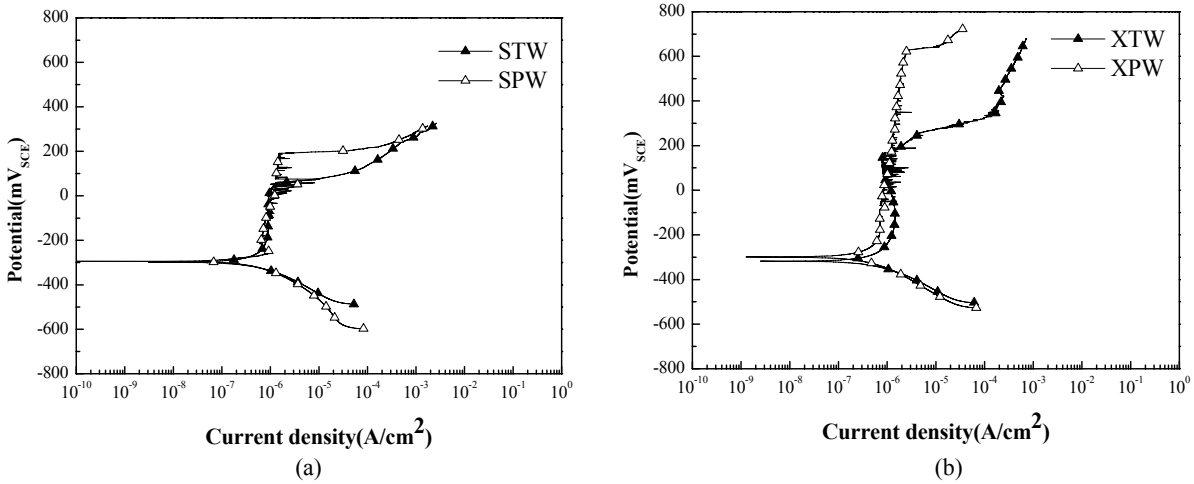

(a) (b)

Fig. 2. Potentiodynamic polarization curves tested in 1M NaCl solution; (a) STS321 (b) XM15J1.

in Table 2 for Cr and in Table 3 for Fe. In the passive film, Cr spectra are composed of Cr metal, Cr_2O_3, $Cr(OH)_3$, CrO_3 and CrO_4^{2-}. Cr^{3+} exists as Cr_2O_3 and $Cr(OH)_3$ which are main oxides of the passive film. Their barrier effect is mainly responsible for the corrosion resistance by preventing the outward diffusion of metal ions through the passive film. Cr^{6+} exists as CrO_3 and CrO_4^{2-} in the passive film.

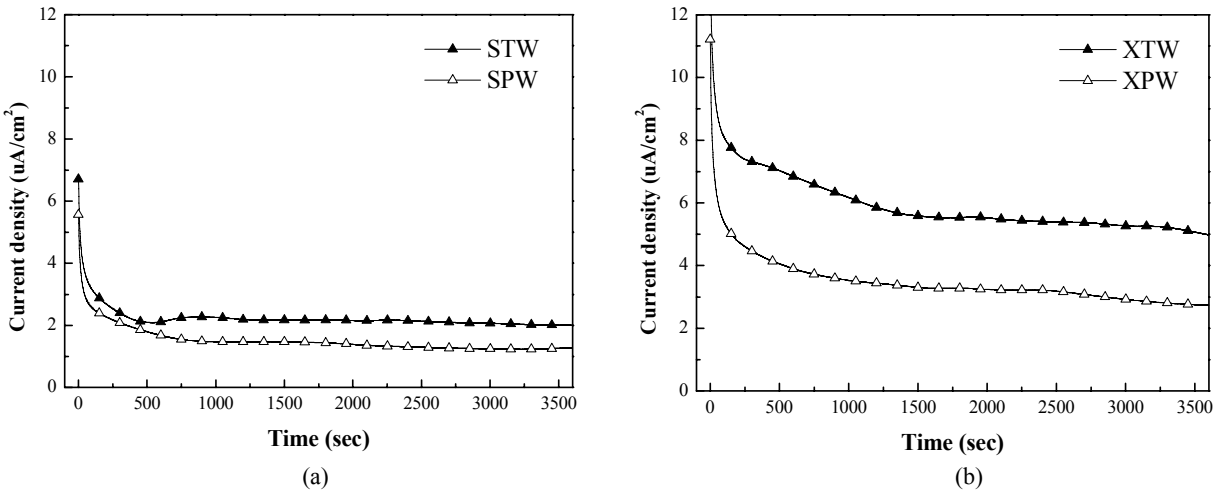

Fig. 3. Potentiostatic polarization curves tested in 1M NaCl solution.

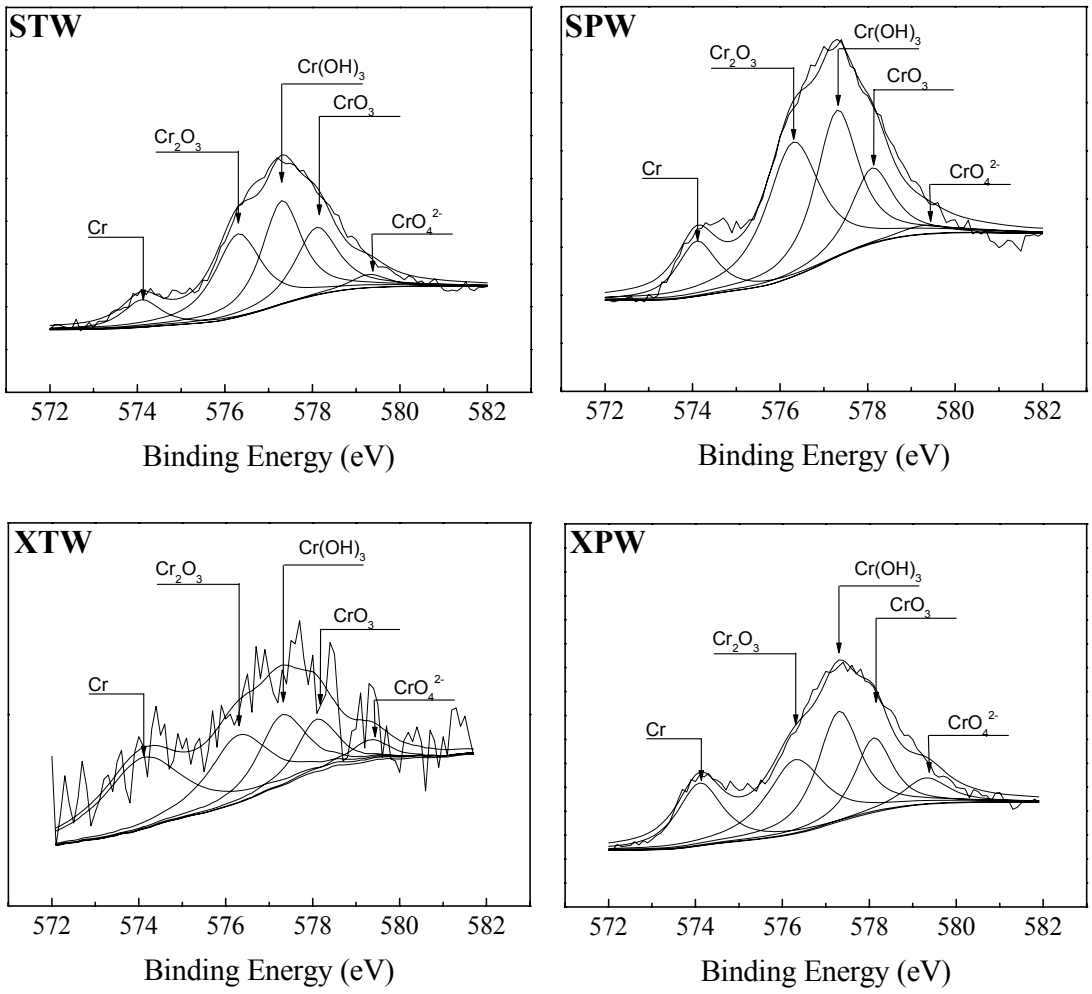

Fig. 4. XPS spectra of Cr at the outermost layer of specimens.

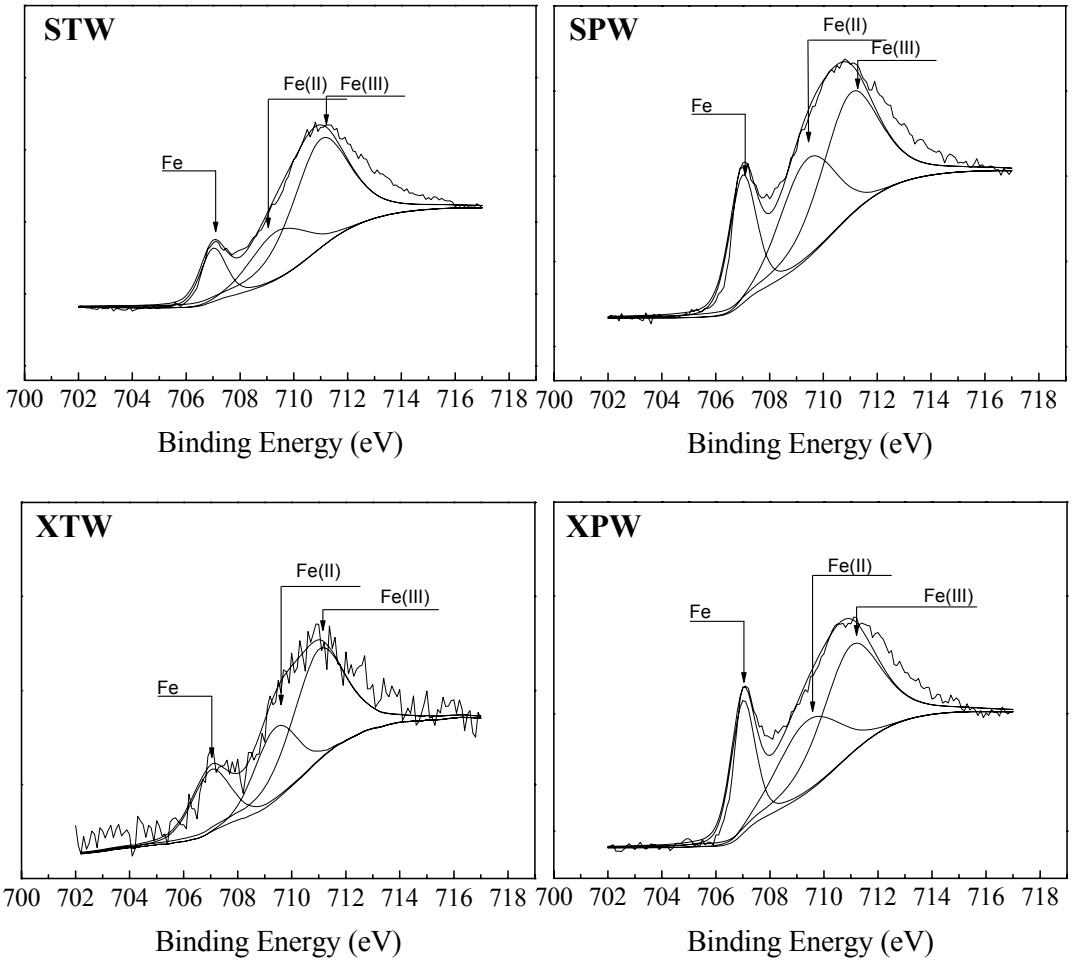

Fig. 5. XPS spectra of Fe at the outermost layer of specimens.

Table 2. Peak area of Cr compounds and $Cr_2O_3/Cr(OH)_3$ ratio for the main spectra of Cr at the outermost layer

	Cr_{met}	Cr_2O_3	$Cr(OH)_3$	CrO_3	CrO_4^{2-}	Cr_2O_3/ $Cr(OH)_3$
STW	7.99	29.97	33.1	22.61	6.33	0.91
SPW	10.32	35.91	27.27	18.61	7.89	1.31
XTW	42.37	22.31	25.69	9.62	0.01	0.86
XPW	17.9	26.83	29.9	17.77	7.6	0.90

Table 3. Peak area of Fe ions and Fe^{2+}/Fe_{met}, Fe^{3+}/Fe_{met} ratio for the main spectra of Fe at the outermost layer

	Fe_{met}	Fe^{2+}	Fe^{3+}	Fe^{2+}/Fe_{met}	Fe^{3+}/Fe_{met}
STW	10.05	29.06	60.89	2.89	6.05
SPW	18.62	36.93	44.45	1.98	2.39
XTW	11.01	33.75	55.24	3.06	5.01
XPW	20.58	32.94	46.48	1.60	2.26

Fe spectra in the passive film are composed of Fe metal, Fe^{2+} and Fe^{3+}. The result suggests that Fe^{3+} is the main component of the passive film since the peak intensity of Fe^{3+} is relatively higher than that of Fe^{2+}.

4. Discussion

In this study, welding method for the flexible tube is one of the most important manufacturing processes since the corrosion resistance of the weldment is greatly dependent on the welding parameters which determine the microstructure of the joint area and consequently the stability of passive film. The main difference in the welding parameter between the TIGW and PAW is the arc type and arc temperature. The arc type is radiation type for TIGW and straight type for PAW. However, the difference in the arc type can be negligible since the thickness of the austenitic stainless steel sheet plate is merely 0.2 mm. On the other hand, the arc temperature is important in the thermody-

namic view point since the undercooling rate is directly related to the arc temperature. The undercooling rate determines the weldment microstructure which is responsible for the mechanical property as well as the corrosion property. The peak arc temperature of PAW is 15,000 ℃ while that of TIGW is 6,000 ℃.[5] Therefore, the undercooling effect is more significant in PAW than in TIGW since the cooling rate of PAW is much higher than that of TIGW.

The undercooling rate determines the ferrite type and its content. In the case of STS321 and XM15J1, ferrite is the primary phase and ferrite to austenite transformation occurs during udercooling.[6),7)] Contrary to the equilibrium phase transformation which can be observed from Fe-Cr-Ni phase diagram, the phase transformation during welding is non-equilibrium, and thus the phase transformation can not be fully completed. When the undercooling rate is high, transformation of the ferrite to austenite is limited and it results in high ferrite content with discontinuous lathy type rather than the continuous vermicular type. Therefore, PAW with high undercooling rate shows high content of ferrite and results in lathy type microstructure. In Fig. 1, the ferrite continuity is lower with PAW than with TIGW.

The image analysis was performed by electrolytic etching in a solution of 50 g NaOH + 100 ml distilled water to evaluate the ferrite content of the weldment and the result is shown in Table 4. The ferrite content is 2.5 ~ 3 % higher in PAW than in TIGW. It is reported that the pitting corrosion resistance becomes high when the ferrite content of weldment is high. This is due to that fact that Cr content is higher in the ferrite phase than in the austenite phase. The higher Cr content contributes better to the stability of passive film.

The bipolar model of the passive film formed on the austenitic stainless steel well explains the protection mechanism by ion selectivity of the passive film.[8)] The bipolar characteristic can be explained by two step ion selectivity. When the inner layer has the anion selectivity and the outer layer has the cation selectivity, in the inner layer of passive film the anion selective space is formed with cations which are getting out of the metal substrate. Then, in the outer layer of passive film $Cr(OH)_3$ is deprotonated to Cr_2O_3 and followed by O^{2-} and H^+. O^{2-} moves from the outer layer to the inner layer due to anion selectivity of inner layer and Cr_2O_3 is formed. The reaction is represented by[9)-11)];

$$\text{Outer layer} : 2Cr(OH)_3 = Cr_2O_3 + 3OH^- + 3H^+$$
$$3OH^- = 3O^{2-} + 3H^+$$

$$\text{Inner layer} : 2Cr_{substrate} + 3O^{2-} = Cr_2O_3 + 6e^-$$

Table 2 shows XPS results of $Cr_2O_3/Cr(OH)_3$ ratio at the outermost layer. $Cr_2O_3/Cr(OH)_3$ ratio is higher with PAW than with TIGW and it is due to the stable Cr_2O_3 passive film formed during PAW.[12)-17)]

Fe diffusion rate is higher than any other ions in stainless steel.[18)] Fe is composed of FeO, Fe_2O_3, $Fe(OH)_3$ in the passive film and exists as $Fe(OH)_3$ at the outer layer because of reaction with H_2O. There are only few cases that a stable passive film can be formed on Fe base alloys, but in most cases Fe oxide is unstable and has low density. It is reported that after inductively coupled plasma-mass spectrometry (ICP-MS) analysis, high amount of Fe followed by Ni and Mo was detected in NaCl solution.[18)] In conclusion, although high diffusion rate of Fe ions, the unstable Fe oxides contribute to low passivity. Table 3 shows that high amount of FeO and $Fe(OH)_3$ at the outermost layer was formed. Table 5 also shows that high growth rate of passive film[19)] with TIGW after potentiostatic test comes from high diffusion rate of Fe ions and may form Fe oxides at the outermost layer. In Fig. 3, the result of potentiostatic test shows that high current density of TIGW comes from dissolution of ions from the passive film. In Fig. 2, the result of potentiodynamic test shows that the lower transpassive potential comes from the breakdown of Fe oxide at the outermost layer.

Table 4. Ferrite content (%) in the weldment

	STW	SPW	XTW	XPW
Ferrite content(%)	3.97	6.42	5.99	8.60

Table 5. Growth rate of passive film determined after potentiostatic test

	STW	SPW	XTW	XPW
Growth rate of passive film	4.75	4.28	9.27	8.55

5. Conclusions

(1) The high cooling rate results in high ferrite content because of difficulty in transformation of ferrite to austenite. High ferrite content of weldment with PAW is observed because of its high cooling rate.

(2) High Cr content in ferrite contributes to the formation of stable passive film. The passive film of PAW at the outermost layer represents high $Cr_2O_3/Cr(OH)_3$ ratio

and low Fe ion/Fe_{met} ratio.

(3) The passive film with high $Cr_2O_3/Cr(OH)_3$ ratio contributes to the corrosion resistance. The passive film with high $Cr_2O_3/Cr(OH)_3$ ratio represents high transpassive potential in the potentiodynamic test and low current density in the potentiostatic test.

References

1. H.H. Uhlig and R.W. Revie, Corrosion and Corrosion Control, N.Y. Wiley (1985).
2. K.Asami, *Corris. Sci*., **18**, 151 (1978).
3. K. Hashimoto, *Corris. Sci*., **19**, 3 (1979).
4. M. G. PUJAR, PhD thesis, Indian Institute of Technology, Bombay (1996).
5. Welding of Stainless Steel, Korean Iron and Steel Association, Seoul, p. 61 (1991).
6. J. M. David and S. A. David, *Weld. J*., **67**, 95 (1988).
7. Mizukami H., Suzuki T., and Umeda T., Tetsu To Hagane, Japan, **77**, 134 (1991).
8. M. Sakashita and N. Sato, Passivity of Metals, p. 740 (1978).
9. Y. C. Lu and C. R. Clayton, *J. Chin. Soc. Corr. Prot*., **18**, 30 (1988) .
10. C. R. Clayton and Y. C. Lu, *J. Electrochem. Soc*., **133**, 2465 (1986).
11. A. R. Brooks, C. R. Clayton, K. Doss, and Y. C. Lu, *J. Electrochem. Soc*., **133**, 2456 (1986).
12. Y. C. Lu, C. R. Clayton, and A. R. Brooks, *Corros. Sci*., **29**, 863 (1989).
13. I. Olefjord, B. Brox, and U. Jelvestam, *J. Electrochem. Soc*., **132**, 2854 (1985).
14. P. Marcus and J. M. Grimal, *Corros. Sci*., **33**, 805 (1992).
15. W. P. Yang, D. Costa, and P. Marcus, *J. Electrochem. Soc*., **141**, 2669 (1994).
16. I. Olefjord and L. Wegrelius, *Corros. Sci*., **31**, 89 (1990).
17. L. Wegrelius, F. Falkenberg, and I. Olefjord, *J. Electrochem. Soc*., **146**, 1397 (1999).
18. P. E. Manning, *Corrosion*, **36**, 246 (1980).
19. C. T. Liu and J. K. Wu, *Corros. Sci*., **49**, 2198 (2007).